Experimental identification of the Inrush safety regions in single-phase power transformers

2024 IEEE International Conference on Electrical Systems for Aircraft, Railway, Ship Propulsion and Road Vehicles & International Transportation Electrification Conference (ESARS-ITEC) | 979-8-3503-7390-5/24/$31.00 ©2024 IEEE | DOI: 10.1109/ESARS-ITEC60450.2024.10819830

Marco Balato
Department of Electrical and Information Technologies (DIETI)
University of Naples Federico II
Via Claudio 21, 80125 Napoli, Italy
marco.balato@unina.it

Antonio Di Pasquale
Department of Electrical and Information Technologies (DIETI)
University of Naples Federico II
Via Claudio 21, 80125 Napoli, Italy
antonio.dipasquale@unina.it

Carmine Stefano Clemente
Department of Medicine and Health Sciences "Vincenzo Tiberio"
University of Molise
Via F. De Sanctis 1, 86100
Campobasso, Italy
carmine.clemente@unimol.it

Annalisa Liccardo
Department of Electrical and Information Technologies (DIETI)
University of Naples Federico II
Via Claudio 21, 80125 Napoli, Italy
annalisa.liccardo@unina.it

Mario Pagano
Department of Electrical and Information Technologies (DIETI)
University of Naples Federico II
Via Claudio 21, 80125 Napoli, Italy
mario.pagano@unina.it

Carlo Petrarca
Department of Electrical and Information Technologies (DIETI)
University of Naples Federico II
Via Claudio 21, 80125 Napoli, Italy
carlo.petrarca@unina.it

Ciro Visone
Department of Electrical and Information Technologies (DIETI)
University of Naples Federico II
Via Claudio 21, 80125 Napoli, Italy
ciro.visone2@unina.it

***Abstract*— This paper investigates the inrush current phenomenon in single-phase power transformers. A suitable experimental setup is designed to identify the locus of the point in the Br $-\theta_0$ plane, called the Inrush Safety Region (ISR), where the inrush current phenomenon does not occur. In particular, it is verified that, for a fixed value of Br, an Inrush Safety Angle Range exists in which the transient current value is comparable with its value in the steady state. This means that, in order to avoid the occurrence of the inrush current phenomenon, it is necessary that the operating point belongs to the ISR. From the above experimental results, it is expected that new inrush current control methods will be developed.**

Keywords*— *Inrush currents, phase diagram, Inrush Safety Regions.

I. INTRODUCTION

The connection of a power transformer to the grid is a critical issue during its lifetime because of the high currents that the device experiences under these conditions. These high currents, commonly known as inrush currents, may be very dangerous as they can cause: i) false operation of the protection devices [1-2]; ii) reduction in transformer lifetime [3-4]; iii) reduce power quality on the system [5-6]. Several methods have been developed to reduce the inrush current, such as series compensator [7,8], sequential phase energization with a grounding resistor [9,10] and controlled switching [11,12]. The most promising of these is controlled switching, which takes into account the mitigating effects of the remanent magnetization (B_r) and the initial phase angle (θ_0). In this kind of approach, the inrush phenomenon is considered as the set of undesirable working points of the power transformer in the $B_r - \theta_0$ plane. Apart from the presence of the undesirable working points, Balato et. al. in [13-14] suggest the existence of a locus of points in the Br $-\theta_0$ plane, called the Inrush Safety operating Region (ISR), in which the inrush phenomenon does not occur. This means that, in order to avoid the occurrence of inrush current phenomenon, it is necessary that the working point of the power transformer belongs to the ISR. The existence of ISR leads to the following assumption: for a fixed value of B_r, there is an inrush safety angle range where the transient current value is comparable to its value at regime condition. The same considerations also apply for the B_r controlled switching. Based on the above considerations, it is clear that two kind of approaches can be used to effectively manage the inrush current in the power transformer: i) θ_0 controlled switching; ii) B_r controlled switching. In both cases, the starting point is the knowledge of the ISR, whose amplitude and position in the $B_r - \theta_0$ plane depend on the circuit and core parameters of the power transformer under consideration. In this paper, an experimental activity has been carried out to identify the ISR with particular reference to single-phase power transformers. The results clearly show that complex hysteresis models are not necessary to estimate the ISR. The above results open up the possibility of developing control techniques that are: robust, easy to implement and time-saving.

II. FAST ESTIMATION THE INRUSH SAFETY REGIONS

The single phase transformer can be modeled by the circuit shown in Figure 2, where the effects of coil resistance and leakage inductance are taken into account by R_s and L_d, respectively. Further the nonlinear mutual inductance represents the transformer frame with open secondary coil. Finally, R_p takes into account the effects of eddy current losses in the ferromagnetic core, while $V_1(t)$ is the voltage AC source. The following equations represent the circuit's model:

$$\dot{\Phi_d} = V_1(t) - \frac{R_{eq}}{L_d}\Phi_d + R_p i_m \quad (1)$$

$$\dot{\Phi_m} = \frac{R_p}{L_d}\Phi_d - R_p i_m \quad (2)$$

$$i_1 = i_p + i_m \quad (3)$$

$$i_1 = \frac{\Phi_d}{L_d} \quad (4)$$

$$i_m = f[\Phi_m] \quad (5)$$

$$V_1(t) = E\sin(\omega t + \theta_0) \quad (6)$$

being $R_{eq} = R_s + R_p$, Φ_d the magnetic leakage flux, Φ_m the magnetic flux linked to the primary coil, while i_m is the primary current.

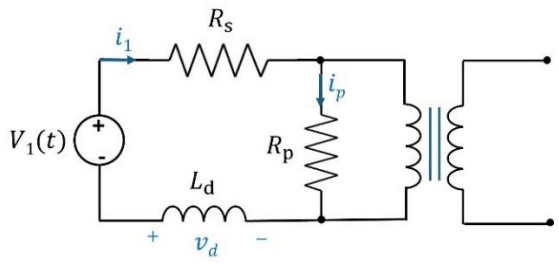

Figure 2. Equivalent circuit of unloaded single-phase transformer.

Moreover, $\Phi_m(t) = NSB(t)$, with B the flux density of the iron core, while $i_m(t) = l/N\ H(t)$, with H(t) the magnetic field. The parameter N gives the primary and secondary turn number of the transformer frame, while S = wp and l = 4h (l=940 mm), represent the core cross section and length of the magnetic circuit, respectively. Tab. I contains the values of the parameters exploited in this analysis.

TABLE I. CORE'S AND CIRCUIT'S PARAMETERS

Description	Symbol	Value
Magnetic saturation	B_s	1.6 T
Coercive field	H_c	270 A/m
Sheet width	w	32.5 mm
Sheet length	h	235 mm
Sheet thickness	p	0.6 mm
Epstein coils turn	N	700
Voltage amplitude	E	4.0 V
Primary coil resistance	R_s	0.56 Ω
Shunt resistance	R_p	40 Ω
Leakage inductance	L_d	1.35 mH
Frequency	f	50 Hz

The above values, as will be shown in Section III, perfectly match the characteristics of the adopted test bench based on the Epstein frame. To estimate the locus of points in which the inrush currents do not arise, that is defined as Inrush Safety Region (ISR), a simplified model can be defined. As described in detail in [13-14], the above model is based on the following assumption:

$$i_m = 0 \qquad \text{if } |\Phi_m| \le \Phi_s \quad (7)$$

Where Φ_s is the magnetic flux at saturation condition. In other words, Eq. (7) means that way from the saturation condition, the primary current may be considered negligible. In this framework, we have that:

$$\Phi_d = \breve{\Phi}\left[\sin(\omega t + \breve{\theta}) - \sin(\breve{\theta})\, e^{-\frac{t}{\tau}}\right] \quad (8)$$

being:

$$\breve{\Phi} = \frac{E\tau}{\sqrt{1+(\omega\tau)^2}} \quad (9)$$

$$\breve{\theta} = \theta_0 - \tan^{-1}(\omega\tau) \quad (10)$$

$$\tau = \frac{L_d}{R_{eq}} \quad (11)$$

and having assumed $\Phi_d(t = 0) = 0$ as initial condition. Finally, by integrating now the second of Eq. (8) the solution for Φ_m reads:

$$\Phi_m = \Phi_r + \frac{V_0}{\omega}\left[\cos\breve{\theta} - \cos(\omega t + \breve{\theta})\right] + V_0\tau\sin(\breve{\theta})\,(e^{-\frac{t}{\tau}} - 1) \quad (12)$$

With $V_0 = \frac{R_p}{R_{eq}}\frac{E}{\sqrt{1+\left(\frac{\omega L_d}{R_{eq}}\right)^2}}$ and $\Phi_r = \Phi_m(0) = NwpB_r$.

The constraints, specified in Eq.(7), takes now the form:

$$\lambda^-(t) \le \frac{\Phi_r}{\Phi_m} \le \lambda^+(t) \quad (13)$$

$$\lambda^-(t) = -1 - \frac{V_0}{\omega\Phi_s}\left[\cos\breve{\theta} - \cos(\omega t + \breve{\theta})\right] - \frac{V_0}{\Phi_s}\tau\sin(\breve{\theta})\,(e^{-\frac{t}{\tau}} - 1) \quad (14)$$

$$\lambda^+(t) = 1 - \frac{V_0}{\omega\Phi_s}\left[\cos\breve{\theta} - \cos(\omega t + \breve{\theta})\right] - \frac{V_0}{\omega\Phi_s}\tau\sin(\breve{\theta})\,(e^{-\frac{t}{\tau}} - 1) \quad (15)$$

Constraints in Eq. (13) are verified for any t if:

$$\sup(\lambda^-) \le \frac{\Phi_r}{\Phi_s} \le \inf(\lambda^+) \quad (16)$$

where:

$$\sup(\lambda^-) = -1 - \frac{V_0}{\omega\Phi_s}\left[\cos\breve{\theta} - 1\right] + \frac{V_0}{\omega\Phi_s}\tau\sin(\breve{\theta}) \quad (17)$$

$$\inf(\lambda^+) = 1 - \frac{V_0}{\omega\Phi_s}\left[\cos\breve{\theta} + 1\right] \quad (18)$$

In Figure 3, the ISR's boundary lines are reported with specific reference to the values shown in the Table I.

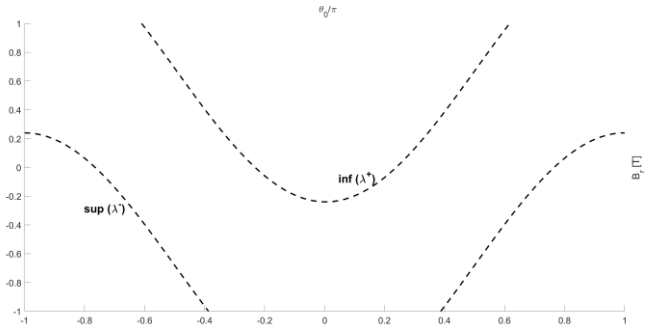

Figure 3. ISR according to simplified model (black curves) in the ($\boldsymbol{\theta_0}$,Br).

III. EXPERIMENTAL RESULTS

The experimental activities have been carried out in the Circuits Laboratory of the Department of Electrical Engineering and Information Technology of University of Naples Federico II, in which an experimental facility has been designed and built. The proposed experimental setup, as shown in Figure 4, consists of: i) Power System (PS), ii) Signal Processing System (SPS).

Power System (PS): A commercial voltage-controlled power supply (Kepco BOP 20-20) has been used as a power generation stadium. The main characteristic of the above device is its capability to provide a sinusoidal output voltage

$V_1(t)$ with tunable amplitude and tunable frequency. To emulate an unloaded power transformer, an Epstein frame has been used. The proposed magnetic circuit consists of four strips with dimensions 32.5 mm × 0.6 mm of a soft ferromagnetic Fe-based alloy, for a total length of the magnetic path of 940 mm. The main core's parameters together with circuit's parameters are reported in Table I.

Signal Processing System (SPS): To manage the experimental data in Matlab® environment (R2024a, Natick, Massachusetts, USA), a modular National Instruments USB system (NI CompactDAQ with NI9215 modules, characterized by 16-bit resolution and maximum sampling frequency of 100 kS/s) has been used. The considered input variables are: the supply voltage ($V_1(t)$); the supply current ($i_1(t)$) and the induced voltage at the secondary winding ($E_2(t)$). In order to describe the inrush currents as a function of initial phase (θ_0) and residual core magnetization (B_r), a proper procedure has been carried out. The above procedure involves two different phases: i) Remanence Phase, ii) Transient Phase.

The SPS output signal ($V_{ref}(t)$) is used to set the amplitude, the frequency and the initial phase (θ_0) of $V_1(t)$. As shown in Figure 5 (a), the time domain behaviour of V_{ref} changes on the basis of the considered working phase. The corresponding hysteresis loops are reported in Figure 5 (b), in which the magnetic remanence point (0, B_r) is shown (green point). Once a specific value of magnetization B_r is attained at the end of the Remanence Phase, the Transient Phase starts with a controllable θ_0. The entire procedure ends when the regime phase is reached. In the experimental campaign two different cases have been considered (Case I and Case II). The above cases differ from the value assumed by B_r. In particular, Case I refers to B_r=723 mT, instead Case II refers to B_r=0 T. As shown in Figure 6, the Inrush Safety Angle Range (θ_{0_ISR}) is obtained by intersecting the line "B_r=B_{r0}" with the boundary lines, defined by applying the Eqs. (17) and (18). In particular:

$$\theta_{0\_ISR\_CASE\ I} = \left[-\pi, -\frac{\pi}{2}\right] \cup \left[\frac{\pi}{2}, \pi\right] \quad (19)$$

$$\theta_{0\_ISR\_CASE\ II} = \left[-\frac{3\pi}{4}, -\frac{\pi}{4}\right] \cup \left[\frac{\pi}{4}, \frac{3\pi}{4}\right] \quad (20)$$

In order to experimentally verify the above theoretical results, three initial phase angles have been considered for both cases: i) $\theta_0 = 0°$ (both cases); ii) $\theta_0 = -135°$ (Case I); iii) $\theta_0 = -170°$ (Case I); iv) $\theta_0 = -60°$ (Case II); v) $\theta_0 = 75°$ (Case II). The experimental results are shown in the Figures 7-12 in which the occurrence of the inrush current is highlighted only when $\theta_0 \notin \theta_{0\_ISR}$ ($\theta_0 = 0°$). In other considered scenarios, the transient current is comparable to its regime value.

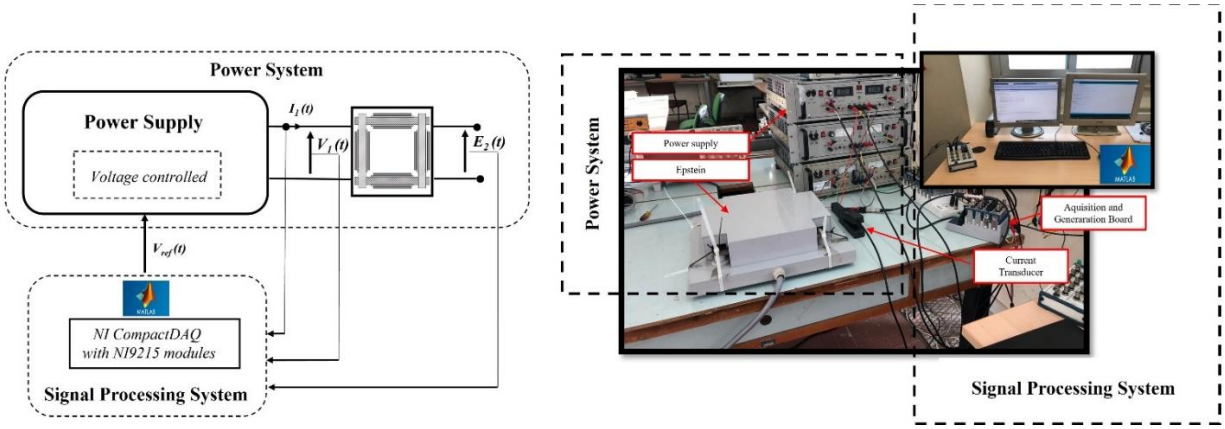

Figure 4. Experimental setup: (a) Block diagram; (b) Snapshot of the experimental facility.

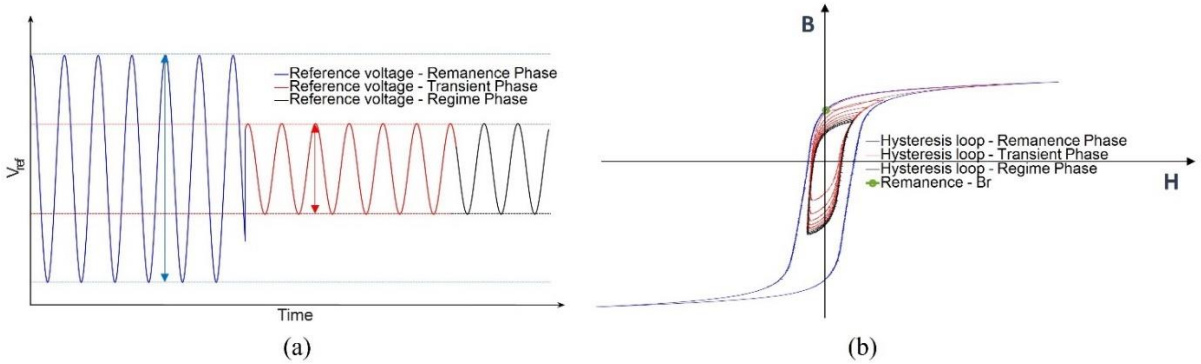

Figure 5. Experimental phases: (a) time behaviour of the output signal $V_{ref}(t)$; (b) Hysteresis branches during the magnetization phase (blue curve) and during the transient phase (red curve).

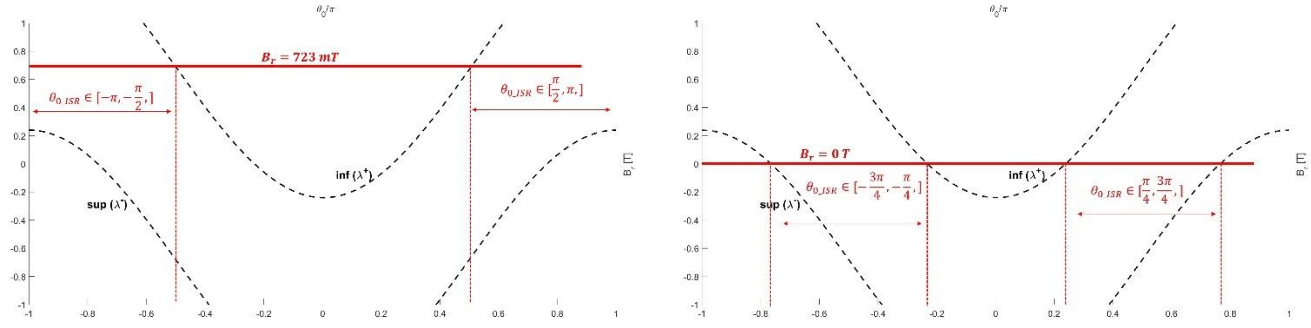

(a) **(b)**

Figure 6. ISR according to simplified model (black curves): (a) Inrush Safety Angle Ranges (CASE I); (b) Inrush Safety Angle Ranges (CASE II).

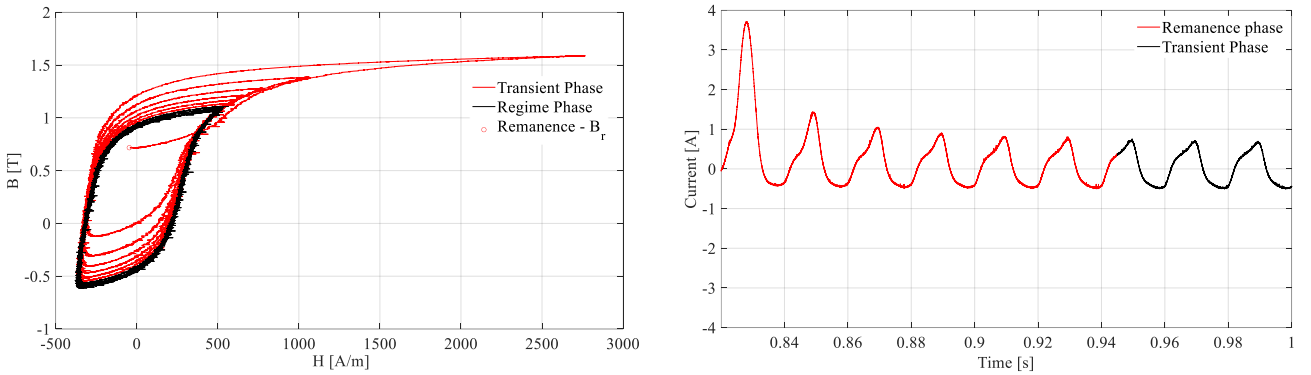

(a) **(b)**

Figure 7. Case I - $\boldsymbol{\theta_0}$ =0°: (a) Hysteresis branches during the transient phase (red curve) and during the regime phase (black curve); (b) time domain behaviour of the input current $i_1(t)$.

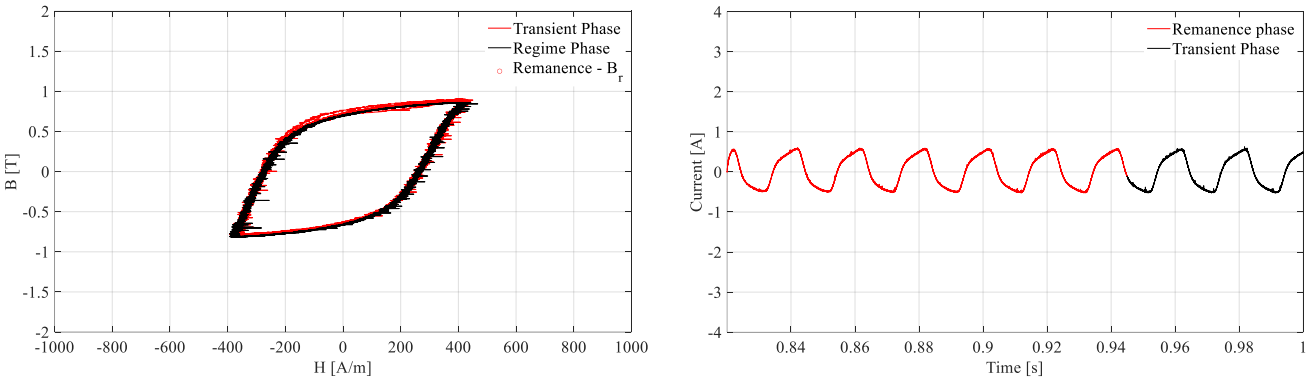

(a) **(b)**

Figure 8. Case I - $\boldsymbol{\theta_0}$ =-135°: (a) Hysteresis branches during the transient phase (red curve) and during the regime phase (black curve); (b) time domain behaviour of the input current $i_1(t)$.

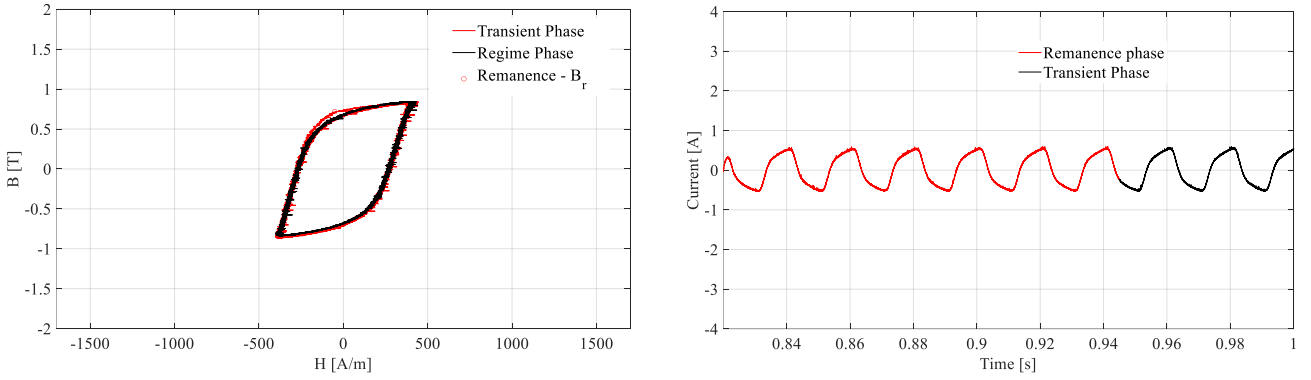

(a) **(b)**

Figure 9. Case I - $\boldsymbol{\theta_0}$ =170°: (a) Hysteresis branches during the transient phase (red curve) and during the regime phase (black curve); (b) time domain behaviour of the input current $I_1(t)$.

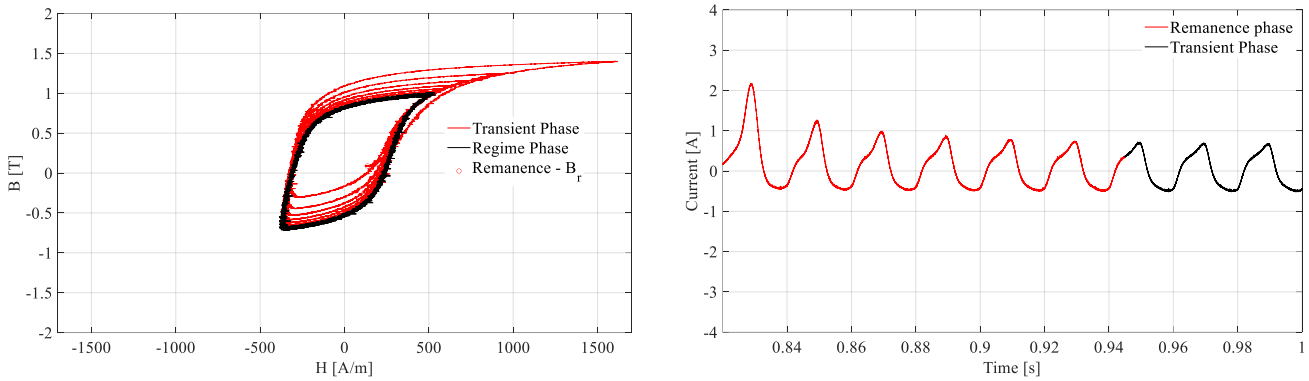

(a) **(b)**

Figure 10. Case II - $\boldsymbol{\theta_0}$ =0°: (a) Hysteresis branches during the transient phase (red curve) and during the regime phase (black curve); (b) time domain behaviour of the input current $i_1(t)$.

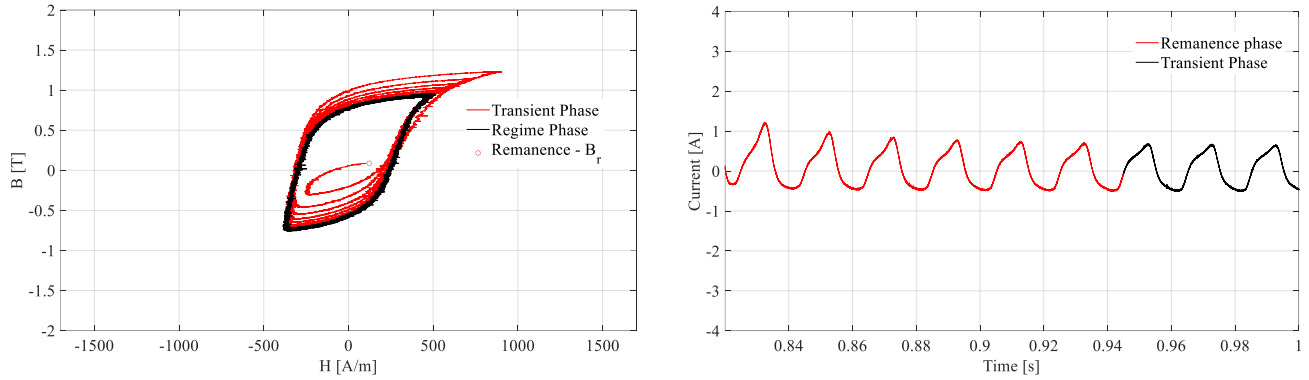

(a) **(b)**

Figure 11. Case II - $\boldsymbol{\theta_0}$ =-60°: (a) Hysteresis branches during the transient phase (red curve) and during the regime phase (black curve); (b) time domain behaviour of the input current $i_1(t)$.

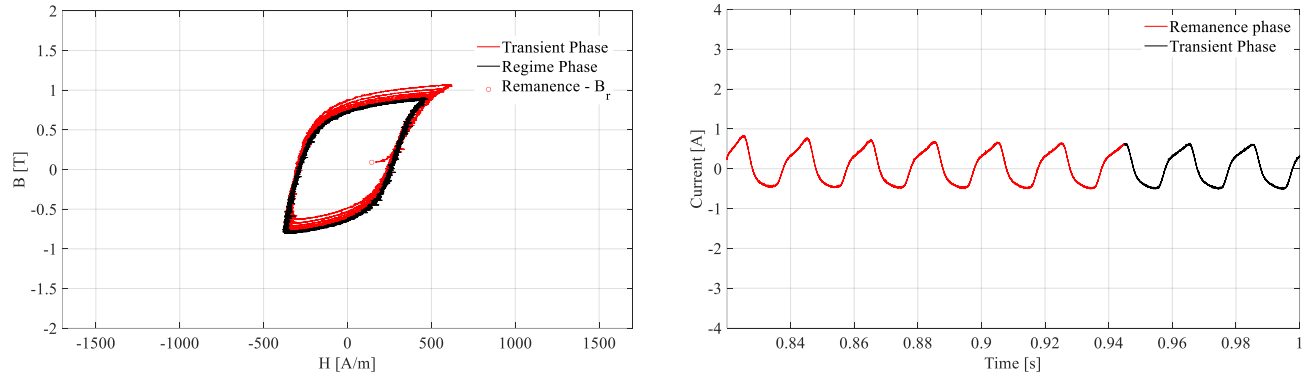

(a) **(b)**

Figure 12. Case II - $\boldsymbol{\theta_0}$ =75°: (a) Hysteresis branches during the transient phase (red curve) and during the regime phase (black curve); (b) time domain behaviour of the input current $i_1(t)$.

IV. Conclusions

In this work the inrush current phenomenon in a single-phase transformer has been investigated. The experimental results confirm the existence of a locus of points in the $Br - \theta_0$ plane, named the Inrush Safety operating Region (ISR), where the inrush phenomenon does not occur. In particular, it has been shown that, for a fixed value of Br (θ_0 controlled scenario), an Inrush Safety Angle Range exists in which the transient current value is comparable with its value at regime condition. The above considerations also apply to the Br controlled scenario. This means that, in order to avoid the occurrence of the inrush current phenomenon, it is necessary that the operating point belongs to the ISR, whose amplitude and position depend on the circuit and core parameters of the transformer under consideration.

References

[1] Ahmed Hosny, Vijay K. Sood, Transformer differential protection with phase angle difference based inrush restraint, Electric Power Systems Research, Volume 115, 2014, Pages 57-64, ISSN 0378-7796, https://doi.org/10.1016/j.epsr.2014.03.027.

[2] R. Hamilton, "Analysis of Transformer Inrush Current and Comparison of Harmonic Restraint Methods in Transformer Protection," in *IEEE Transactions on Industry Applications*, vol. 49, no. 4, pp. 1890-1899, July-Aug. 2013, doi: 10.1109/TIA.2013.2257155.

[3] M. Steurer and K. Frohlich, "The impact of inrush currents on the mechanical stress of high voltage power transformer coils," in *IEEE*

Transactions on Power Delivery, vol. 17, no. 1, pp. 155-160, Jan. 2002, doi: 10.1109/61.974203.

[4] W. Neves *et al*., "A comparative investigation of electromechanical stresses on transformers caused by inrush and short-circuit currents," *11th International Conference on Electrical Power Quality and Utilisation*, Lisbon, Portugal, 2011, pp. 1-6, doi: 10.1109/EPQU.2011.6128805.

[5] M. Nagpal, T. G. Martinich, A. Moshref, K. Morison and P. Kundur, "Assessing and limiting impact of transformer inrush current on power quality," in *IEEE Transactions on Power Delivery*, vol. 21, no. 2, pp. 890-896, April 2006, doi: 10.1109/TPWRD.2005.858782.

[6] L. F. Blume, G. Camilli, S. B. Farnham and H. A. Peterson, "Transformer magnetizing inrush currents and influence on system operation," in *Electrical Engineering*, vol. 63, no. 6, pp. 366-374, June 1944, doi: 10.1109/EE.1944.6440312.

[7] J. C. Oliveira, C. E. Tavares, R. Apolonio, A. B. Vasconcellos and H. S. Bronzeado, "Transformer Controlled Switching to Eliminate Inrush Current - Part I: Theory and Laboratory Validation," *2006 IEEE/PES Transmission & Distribution Conference and Exposition: Latin America*, Caracas, Venezuela, 2006, pp. 1-5, doi: 10.1109/TDCLA.2006.311523.

[8] Hsu-Ting Tseng, Jiann-Fuh Chen, Bidirectional impedance-type transformer inrush current limiter, Electric Power Systems Research, Volume 104, 2013, Pages 193-206, ISSN 0378-7796, https://doi.org/10.1016/j.epsr.2013.06.007.

[9] A. Ketabi and Ali Reza Hadidi Zavareh, "New method for inrush current mitigation using series voltage-source PWM converter for three phase transformer," *2011 2nd Power Electronics, Drive Systems and Technologies Conference*, Tehran, Iran, 2011, pp. 501-506, doi: 10.1109/PEDSTC.2011.5742470.

[10] Wilsun Xu, S. Abdulsalam, Yu Cui and Xian Liu, "A sequential phase energization technique for transformer inrush current reduction part II: theoretical analysis and design guide," *IEEE Power Engineering Society General Meeting, 2004.*, Denver, CO, USA, 2004, pp. 534 Vol.1-, doi: 10.1109/PES.2004.1372856.

[11] S. G. Abdulsalam and W. Xu, "A Sequential Phase Energization Method for Transformer Inrush Current Reduction—Transient Performance and Practical Considerations," in *IEEE Transactions on Power Delivery*, vol. 22, no. 1, pp. 208-216, Jan. 2007, doi: 10.1109/TPWRD.2006.881450.

[12] J. H. Brunke and K. J. Frohlich, "Elimination of transformer inrush currents by controlled switching. II. Application and performance considerations," in *IEEE Transactions on Power Delivery*, vol. 16, no. 2, pp. 281-285, April 2001, doi: 10.1109/61.915496.

[13] László Prikler, György Bánfai, Gábor Bán, Péter Becker, Reducing the magnetizing inrush current by means of controlled energization and de-energization of large power transformers, Electric Power Systems Research, Volume 76, Issue 8, 2006, Pages 642-649, ISSN 0378-7796, https://doi.org/10.1016/j.epsr.2005.12.022.

[14] M. Balato, S. Perna, C. Petrarca, and C. Visone, “A simple scheme for the inversion of a preisach like hysteresis operator in saturation conditions,” AIP Advances, vol. 12, no. 3, p. 035047, 2022.

[15] M. Balato, S. Perna, C. Petrarca, and C. Visone, “Piecewise linear modeling for Inrush Safety Regions detection and its validation through a Preisach model and experimental data,” in *IEEE Transactions on Magnetics*, vol. 59, no. 8, pp. 1-9, Aug. 2023, Art no. 8400609, doi: 10.1109/TMAG.2023.3279583.